Biogeosciences Discuss., 11, 9667–9695, 2014
www.biogeosciences-discuss.net/11/9667/2014/
doi:10.5194/bgd-11-9667-2014

Biogeosciences Discussions
Open Access

Implications of carbon saturation model structure for simulated nitrogen mineralization dynamics

C. M. White[1], **A. R. Kemanian**[2], **and J. P. Kaye**[1]

[1]Department of Ecosystem Science and Management, The Pennsylvania State University, 116 Agricultural Sciences and Industries Building, University Park, PA 16802, USA
[2]Department of Plant Science, The Pennsylvania State University, 116 Agricultural Sciences and Industries Building, University Park, PA 16802, USA

Received: 17 April 2014 – Accepted: 28 May 2014 – Published: 20 June 2014

Correspondence to: C. M. White (cmw29@psu.edu)

Published by Copernicus Publications on behalf of the European Geosciences Union.

Abstract

Carbon (C) saturation theory suggests that soils have a limited capacity to stabilize organic C and that this capacity may be regulated by intrinsic soil properties such as clay content and mineralogy. While C saturation theory has advanced our ability to predict soil C stabilization, we only have a weak understanding of how C saturation affects N cycling. In biogeochemical models, C and N cycling are tightly coupled, with C decomposition and respiration driving N mineralization. Thus, changing model structures from non-saturation to C saturation dynamics can change simulated N dynamics. Carbon saturation models proposed in the literature calculate a theoretical maximum C storage capacity of saturating pools based on intrinsic soil properties, such as clay content. The extent to which current C stocks fill the storage capacity of the pool is termed the C saturation ratio, and this ratio is used to regulate either the efficiency or the rate of C transfer from donor to receiving pools. In this study, we evaluated how the method of implementing C saturation and the number of pools in a model affected net N mineralization from decomposing plant residues. In models that use the C saturation ratio to regulate transfer efficiency, C saturation affected N mineralization, while in those in which the C saturation ratio regulates transfer rates, N mineralization was independent of C saturation. When C saturation ratio regulates transfer efficiency, as the saturation ratio increases, the threshold C : N ratio at which positive net N mineralization occurs also increases because more of the C in the residue is respired. In a single-pool model where C saturation ratio regulated the transfer efficiency, predictions of N mineralization from residue inputs were unrealistically high, missing the cycle of N immobilization and mineralization typically seen after the addition of high C : N inputs to soils. A more realistic simulation of N mineralization was achieved simply by adding a second pool to the model to represent short-term storage and turnover of C and N in microbial biomass. These findings increase our understanding of how to couple C saturation and N mineralization models, while offering new hypotheses about the relationship between C saturation and N mineralization that can be tested empirically.

BGD
11, 9667–9695, 2014

1 Introduction

Over the last two decades, the development of carbon (C) saturation theory has fundamentally changed our understanding of C storage in soils and new biogeochemical models have been developed to include C saturation dynamics (Hassink and Whitmore, 1997; Kemanian et al., 2005; Stewart et al., 2007; Kemanian et al., 2011). In biogeochemical models that couple C and nitrogen (N) cycles, C fluxes drive N mineralization (Manzoni and Porporato, 2009). Thus, altering the structure of the C model to accommodate saturation dynamics is likely to affect the coupled N cycle. Yet, few attempts have been made to understand how C saturation affects N cycling (e.g. Castellano et al., 2012). In particular, little attention has been given to how the C saturation models proposed in the literature affect N mineralization dynamics in coupled biogeochemical models.

The majority of ecosystem scale biogeochemical models that couple C and N cycles use linear C models with no saturation (Manzoni and Porporato, 2009). In these models, C decomposition occurs with first-order kinetics and steady-state C levels will increase linearly as C inputs increase. In C saturation models, however, steady-state C levels will approach an asymptotic limit as C inputs increase. Both non-saturation and saturation C models couple N mineralization and immobilization ($N_{m\text{-}imm}$) to C decomposition (C_{dec}) through the stoichiometry of the decomposing ($C:N_{dec}$) and receiving ($C:N_{rec}$) pools and the C transfer efficiency between pools (i.e. the quotient of the transferred to decomposed C mass, ε, g C g^{-1} C). This coupling is represented as:

$$N_{m\text{-}imm} = C_{dec}\left(\frac{1}{C:N_{dec}} - \frac{\varepsilon}{C:N_{rec}}\right) \quad (1)$$

The coupling of C and N described by Eq. (1) creates a relationship between C saturation and N mineralization that depends on the structure of the C saturation model. For instance, one way to implement C saturation dynamics is by regulating ε as a function of the C saturation ratio (the ratio of the current C to that of a putative maximum

BGD
11, 9667–9695, 2014

C level of the saturating pool) (Stewart et al., 2007; Kemanian et al., 2011) (Fig. 1a). Alternatively, the C saturation ratio can regulate the decomposition rate (k, T^{-1}) of the pool feeding the saturating pool (Hassink and Whitmore, 1997) (Fig. 1b). In these models, when the saturation ratio increases, ε and k decrease. These two methods of implementing C saturation dynamics create explicit coupling between C saturation and N mineralization dynamics in different ways, the implications of which have not been explored.

The N mineralization in Eq. (1) applies to any transfer of C and N between pools. The extent to which net N mineralization occurs as opposed to net N immobilization depends on the magnitude of ε and the difference between $C:N_{dec}$ and $C:N_{rec}$. The $C:N$ of decomposing plant residue can vary widely across residue types. The critical $C:N$ ($C:N_{cr}$) below which decomposing residue will cause positive net N mineralization can be solved using Eq. (1) when $N_{m\text{-}imm} = 0$, as shown in Eq. (2).

$$C:N_{cr} = \frac{C:N_{rec}}{\varepsilon} \tag{2}$$

This equation shows that a decrease in ε will increase $C:N_{cr}$. For example, if the receiving pool is saturated, the $C:N_{cr}$ of decomposing substrates increases. The biological meaning of a decreasing ε is that a smaller fraction of the products of microbial decomposition stabilize in organo-mineral associations and thus remain available for microbial use. It is important to recognize that the $C:N_{cr}$ in Eq. (2) is for a simple transfer and not for the sum of all transfers in a whole soil. A simple transfer may immobilize N while a simultaneous transfer among different pools in the soil may result in net N mineralization at the whole soil level.

Although the coupling of C and N cycles in soils is largely mediated by microbial biomass, the microbial pool has been given little consideration in saturation models. In only one case is the microbial pool explicitly represented in the model structure (Hassink and Whitmore, 1997). In other cases the microbial pool is either not included (Stewart et al., 2007) or is implicitly included when parameterizing ε (Kemanian et al., 2011). In the latter model, ε lumps in one step what is a cascade of C transfers among

BGD
11, 9667–9695, 2014

pools mediated by microbial turnover. While this approach may produce reasonable results for net C exchange in monthly or yearly time frames, when these ε are used for short time steps they may obscure the N cycling during microbial turnover.

A feature that implicitly links non-saturation and saturation C models is the role of soil clay concentration (f_{clay}, g clay g^{-1} soil) in mediating ε, and hence N mineralization. In C saturation models, f_{clay} is used to calculate the maximum size of the saturating pool (Hassink and Whitmore, 1997; Kemanian et al., 2011), thus the C saturation ratio is a function of f_{clay}. Models that use the C saturation ratio to regulate ε connect f_{clay} to ε. Carbon models have long used f_{clay} to directly regulate ε (Parton et al., 1987; Jenkinson, 1990; Verberne et al., 1990) in a way that leads to lower N mineralization rates and a lower $C:N_{cr}$ in clay-rich soils. This method originated from observations that soils with high f_{clay} stabilize a greater proportion of C inputs. For example, Jenkinson (1990) and Parton et al. (1987) used relationships derived from Sørensen (1975) and Sørensen (1981). However, Hassink (1996) found that the C saturation ratio of a soil was a better predictor of C retention than f_{clay}, a finding that suggests both, that N cycling can be similar with f_{clay}-based or C saturation-based control of ε, and that C saturation may be a more fundamental mechanism to integrate the effect of soil texture in a coupled C and N model. Yet, whether non-saturation and saturation models differ in their representation of N cycling has not been fully explored.

In summary, linking N dynamics and C saturation theory is relevant and currently this linkage is poorly understood in conceptual and quantitative biogeochemical models. To advance this linkage, we hypothesize that the structure and parameterization of different C models will affect the dynamics of a coupled N mineralization model. Specifically, we propose that each model will have characteristic N mineralization-immobilization dynamics that will reflect both the model structure and the consideration or not of C saturation. To test this hypothesis, we compared four model structures (Fig. 2). These model structures were taken from the literature or developed for this investigation. Models varied in whether C saturation regulated either ε or k and in the number of C pools included in the model. We coupled N to C cycling to obtain N mineralization and il-

BGD
11, 9667–9695, 2014

lustrate how the C model structure affects the $C:N_{cr}$ and the temporal dynamics of a simulated inorganic N pool during plant residue decomposition.

2 Methods

2.1 Structure of the carbon models

We focused on three C saturation model structures and one non-saturation C model (Fig. 2). The first and simplest model in our study is a single-pool saturation model, adapted from the models proposed by Kemanian et al. (2005, 2011) and Stewart et al. (2007). The second model expands the single-pool saturation model by adding a microbial pool (C_m). We termed this model the microbial saturation model to reflect the explicit inclusion of a microbial pool through which C and N must pass. The third model is the abiotic saturation model, whose structure was proposed by Hassink and Whitmore (1997). This model includes a microbial pool (C_m), a labile unprotected pool (C_{un}), and a saturating pool of protected C (C_s). We called this the abiotic saturation model because the saturating pool is directly linked to the labile pool and any transfers are abiotic sorption and desorption. We compared these three C saturation models to the Rothamsted C (RothC) model (Jenkinson, 1990), which is based on first order kinetics and results in a linear relationship between C input and steady-state C level.

We parameterized the turnover rate of the pools to return similar steady-state C stocks using as benchmark the steady-state C and the rates in RothC. The turnover rate of soil C (k_s) in the single-pool saturation model and that of microbial C (k_m) in the microbial and abiotic saturation models are taken from RothC. In the microbial and abiotic saturation models, k_s is derived such that steady-state C_s levels in these models will be equivalent to steady-state C_s in the single-pool saturation model. The residue C pool turnover rate (k_r) in the saturation models is taken as the weighted average of the turnover rates for decomposable (k_{dpm}) and resistant (k_{rpm}) plant material input pools in RothC (i.e., $0.59k_{dpm} + 0.41k_{rpm}$). Model structures are diagrammed in Fig. 2,

BGD
11, 9667–9695, 2014

parameters are specified in Table 1, and the differential equations for each pool are in Table 2.

2.1.1 Single-pool saturation model

In the single-pool saturation model, decomposed C from the pool of residue inputs (C_r) is transferred directly to C_s. The ε from C_r to C_s is regulated by an efficiency factor (ε_x) and the saturation ratio, C_s/C_x, where C_x is the maximum C storage capacity. We calculate C_x as a function of the soil clay fraction (f_{clay}) using the formula developed by Hassink and Whitmore (1997). In this model, ε_x represents a humification coefficient (sensu Hénin and Dupuis, 1945), or the slope that would be obtained by regressing dC_s/dt against C inputs. This coefficient is an effective efficiency that lumps the C use efficiency of the microbes feeding on residues and on microbial biomass (predation), detritus and exudates. We used $\varepsilon_x = 0.18\,g\,C\,g^{-1}$ C. This value is in the upper range reported by Huggins et al. (1998), and would correspond to three cycles of microbial feeding with a C use efficiency of $0.56\,g\,C\,g^{-1}$ C (i.e., 0.56^3). This C use efficiency agrees well with a representative upper value in soils reported in Fig. 6 of Manzoni et al. (2012). Both C_r and C_s decay with first order kinetics according to the rate constants in Table 1. Decomposed C that is not transferred to C_s is respired as CO_2.

2.1.2 Microbial saturation model

In the microbial saturation model, C decomposed from C_r and C_s is transferred to C_m while C decomposed from C_m is transferred to C_s. The ε from decomposing pools to receiving pools is calculated as the square root of the ε used in the single-pool saturation model. Thus, C that is stepping from C_r to C_m and from C_m to C_s is retained with an overall efficiency similar to the single-pool model. Decomposed C that is not transferred to a receiving pool is respired as CO_2. The three pools C_r, C_m, and C_s decay with first order kinetics. The turnover rates k_r and k_m are consistent with the

BGD
11, 9667–9695, 2014

other models while k_s is derived to maintain a steady state C_s level that is equivalent to the single-pool saturation model. The derivation for k_s is provided in Appendix A.

2.1.3 Abiotic saturation model

The abiotic saturation model is adapted from the structure proposed by Hassink and Whitmore (1997). Decomposed C from C_r and C_{un} is transferred to C_m with a fixed ε representing microbial C use efficiency. Carbon in C_{un} is also transferred to C_s, a protected pool, simulating the abiotic sorption of organic C to mineral surfaces. The transfer rate from C_{un} to C_s ($k_{un\text{-}s}$) is controlled by a maximum rate that is regulated by the size of C_s relative to its maximum capacity (C_x). C_x is calculated as a function of f_{clay} using the original linear regression developed by Hassink and Whitmore. Transfer of C from C_s to C_{un}, representing the desorption of organic C from the mineral phase, occurs at the rate k_s. Because the sorption-desportion process is abiotic, the ε between C_{un} and C_s is 1 (no CO_2 is respired in the transfer). The decay rates k_r and k_m are consistent with the other models. We set the default value for the decay rate k_{un} at 0.01 while the decay rates $k_{un\text{-}s}$ and k_s were derived such that steady state C_s level would be equivalent to the single-pool saturation model (see Appendix A for the derivation).

2.1.4 Rothamsted C model

In the RothC model (Jenkinson, 1990), C pools include decomposable (C_{dpm}) and resistant (C_{rpm}) fractions of plant material inputs, and microbial (C_m) and stabilized (C_s) pools of soil C. Each pool decays with its own first-order rate constant. Decomposed C from each pool is transferred to the receiving pools with an efficiency (ε) that is determined by f_{clay}. This efficiency varies from a low of 0.15 at 1 % clay content to a plateau of approximately 0.24 at 45 % clay content. The fraction of decomposed C that is not transferred to a receiving pool ($1 - \varepsilon$) is respired as CO_2. Of the total C decomposed from all pools and not lost as CO_2, 54 % is transferred to C_s and 46 % is transferred to C_m.

BGD
11, 9667–9695, 2014

2.2 Modeling N mineralization

We coupled C and N cycling using the simple model for N mineralization described in Eq. (1). In this N mineralization model, N decomposes from the donor pool in proportion to C decomposition based on the $C:N_{dec}$. A portion of the decomposed C is transferred to a receiving pool based on ε, while the remaining C is respired as CO_2. Decomposed organic N is transferred to the receiving pool in proportion to the C received by the pool based on the $C:N_{rec}$. Nitrogen mineralization (or immobilization) is calculated as the difference between the N decomposed and the N assimilated by the receiving compartment. Nitrogen mineralized as a result of C decomposition is added to an inorganic N (N_i) pool. When $N_{m\text{-}imm}$ is negative, immobilization occurs and N is removed from the N_i pool. If the pool size of N_i is insufficient to meet the immobilization demand, C decomposition is limited by N availability, as we assume that ε will not change. Under such circumstances, we calculate the reduced C decomposition by rearranging Eq. (1) and assuming that $N_i + N_{m\text{-}imm} = 0$, which yields the following equation:

$$C_{dec} = \frac{N_i}{\frac{\varepsilon}{C:N_{rec}} - \frac{1}{C:N_{dec}}} \tag{11}$$

We used a fixed C : N of 10 for the microbial and soil organic matter pools while the C : N of the input residues was an input parameter to the model.

2.3 Modeling exercises

To study and illustrate the differences in C and N cycling among the four models and the implications of the C model structure on N mineralization we did the following: (i) derived the analytical solutions to the steady-state size of each C pool as a function of C input level for all models; (ii) calculated the $C:N_{cr}$ for a range of clay and saturation ratios; and (iii) simulated the temporal dynamics of N mineralization at a daily time-step following a one-time residue addition.

BGD
11, 9667–9695, 2014

In the daily time-step residue addition simulation, a 5 Mg C ha^{-1} mass of plant residues with a C : N of 60 added to the soil on day 1 was allowed to decompose for 365 days. Nitrogen mineralization and/or immobilization resulting from residue and soil organic matter decomposition was added to or removed from the N_i pool. The simulation was conducted for 5 % clay and 25 % clay soils. Soil organic C pool sizes in each model were initialized to steady-state levels for an annual plant residue addition level of 5 Mg C ha^{-1}. The N_i pool was initialized to a size of 0.05 Mg N ha^{-1}. Simulations were conducted in Microsoft Excel using the Visual Basic for Applications programming language.

3 Results

3.1 Characteristics and behavior of the C models

As expected, steady-state levels of C pools in each model responded to increasing C inputs in either a saturating or linear manner depending on the model structure (Table 3 and Fig. 3). The C_s pool saturates in all three saturation models and C_m saturates in the microbial saturation model. In all other instances, the C pools respond linearly to increasing C inputs.

The f_{clay} regulates C storage in both the saturation models and the RothC model, though through different mechanisms. In the saturation models, f_{clay} is used to calculate the parameter C_x, which appears in the analytical solution of steady-state C_s in all three saturation models and steady-state C_m in the microbial saturation model. In RothC f_{clay} is used to calculate the transfer efficiency ε, which appears in the steady state analytical solution of C_s and C_m. For these pools, soils with more clay will have a greater steady-state C storage owing to increases in either C_x (saturation models) or ε (RothC) (Fig. 3).

When C input levels and soil clay concentration were low, only small differences in total C storage were predicted by each model, as calculated by summing the C

BGD
11, 9667–9695, 2014

mass of all SOC pools (Fig. 3c and 3d). However, at higher C input levels and soil clay content, large divergences between the saturation models and the non-saturation model occurred owing to the asymptotic characteristic of saturation models. Even though the abiotic saturation model contained the non-saturating pools C_{un} and C_m, the overall response of total C storage to increasing C inputs was similar to that of a pure saturation model. This is because of the relatively small size of the C_{un} and C_m pools compared to C_s when C inputs are within the range typical of most ecosystems ($< 15\,\mathrm{Mg\,C\,ha^{-1}\,yr^{-1}}$).

3.2 Nitrogen mineralization

Carbon model structure affected the coupling of C saturation and N mineralization based on the method that was used to implement C saturation dynamics. In models that use the C saturation ratio to regulate the C transfer efficiency (ε), as in the single-pool and microbial saturation models, increasing the C saturation ratio increased N mineralization. When the C saturation ratio regulates the transfer rate (k), as in the abiotic saturation model, C saturation had no effect on N mineralization.

We calculated the analytical solution to $C:N_{cr}$ for each model by substituting the parameterization of ε for each model into Eq. (2) (Table 4). In the single-pool and microbial saturation models, $C:N_{cr}$ is a function of C_s/C_x, the C saturation ratio. As the saturation ratio increases, $C:N_{cr}$ increases gradually at first and then more sharply as C_s/C_x becomes greater than 0.6 (Fig. 4a). The single-pool saturation model always predicts a higher $C:N_{cr}$ than the microbial saturation model and the divergence increases as the saturation ratio increases. In the abiotic saturation model, on the other hand, the saturation ratio does not affect the efficiency with which decomposing C is retained by the microbial pool, so $C:N_{cr}$ is a fixed value based on the growth efficiency (ε) of the microbial pool.

Although RothC does not include C saturation, it does regulate C transfer efficiency to the microbial pool based on f_{clay}. Thus we sought to compare how f_{clay} affects $C:N_{cr}$ for each model using the analytical solutions in Table 4. In the single-pool and micro-

BGD
11, 9667–9695, 2014

bial saturation models we held C_s constant at 32 Mg C ha^{-1} while C_x varied with f_{clay}. In RothC, ε varied with f_{clay}. As f_{clay} increased, C : N_{cr} decreased in the single-pool saturation, microbial saturation, and RothC models (Fig. 4b), though the effect was smallest for the microbial saturation model. In the abiotic saturation model, f_{clay} had no effect on C : N_{cr}.

The method in which each model calculates ε also affects N mineralization rates, as can be seen by the simple N mineralization model described in Eq. (1). To characterize how each model structure affects the temporal dynamics of N mineralization, we simulated a plant residue addition of 5 Mg C ha^{-1} with a C : N of 60, modeling decomposition and N mineralization at a daily time-step for one year. In the simulation, organic C and N pool sizes were initialized to steady-state levels. Therefore, for all the models, the total N mineralized at the end of one year was equal to the quantity of organic N inputs. Nonetheless, we found contrasting patterns across models in the temporal dynamics of N mineralization over the one-year simulation (Fig. 5). With a 5 % clay soil, both the single-pool saturation model and RothC resulted in immediate net N mineralization following the residue addition. The microbial and abiotic saturation models both resulted in a period of net N immobilization following the residue addition with the microbial model showing a greater level and longer period of immobilization than the abiotic model. With a 25 % clay soil, the single-pool saturation model still resulted in immediate mineralization while RothC shifted to a small level of immobilization for a brief period. In the microbial saturation model, the level and duration of N immobilization increased slightly with a 25 % clay soil compared to the 5 % clay soil. Mineralization dynamics in the abiotic saturation model were not affected by soil clay content.

4 Discussion

A significant result from our work is that despite similar predictions of C storage across the saturation models, dynamics of N mineralization diverged widely due to the structure of each model. We revealed two important considerations for how C saturation

BGD
11, 9667–9695, 2014

models can be linked to N mineralization dynamics. First, a single-pool C saturation model that may predict long-term C storage well can misrepresent short-term N mineralization if N cycling is simply linked to the long cadence of C cycling. This mismatch between C and N cycling can be greatly improved by simply adding an intermediate pool of microbial biomass through which C and N must pass; an addition that does not affect long term C cycling. Second, the influence of C saturation on N mineralization dynamics depends on whether C saturation is modeled as a process regulating transfer efficiencies or a process regulating transfer rates. These findings suggest appropriate ways to structure coupled models of C saturation and N mineralization and offer new hypotheses about the links between C saturation and N mineralization processes that should be tested with further research.

4.1 Temporal scale and N mineralization dynamics

The four models we compared each affected N mineralization dynamics differently due to the parameterization of the C transfer efficiency (ε) used in Eq. (1). The single-pool saturation model uses an effective efficiency that lumps approximately three cycles of microbial predation into one step. This approach has been used to accurately predict C storage over decadal time scales (Kemanian and Stöckle, 2010) and a single-pool model offers the advantages of parsimony (Stewart et al., 2007) and simplicity of calibration requirements (Kemanian and Stöckle, 2010). When coupled to a model of N mineralization, however, the single-pool saturation model yielded a $C:N_{cr}$ that ranged from 55 to over 555 as the C saturation ratio rose above 0.9. This range of $C:N_{cr}$ is above the range that has been observed across a variety of ecosystem and substrate types except for woody residue substrates (Manzoni et al., 2008).

In the single-pool saturation model, the steepness of the rise in $C:N_{cr}$ as C saturation ratio increases could be tempered by exponentiating the C saturation ratio. For example, Kemanian et al. (2011) raised the C saturation ratio to the sixth power. While this method may maintain $C:N_{cr}$ at more reasonable levels across a broader range of

BGD
11, 9667–9695, 2014

C saturation ratios, it only shifts the sharp rise in $C:N_{cr}$ to a higher saturation ratio and accentuates the steepness of the rise when it does occur.

A simple modification to the single-pool saturation model, adding an intermediate pool representative of microbial biomass, greatly improved the dynamics of N mineralization. In the microbial saturation model, $C:N_{cr}$ ranged from 23 to over 74 as the C saturation ratio rose above 0.9. A similar range of $C:N_{cr}$ values was observed in non-woody plant residues by Manzoni et al. (2010), though the range was mostly explained by N concentration of the residues rather than C saturation of the soil. Within C saturation ratios that would occur under a more realistic C input level ($\sim 5\,Mg\,C\,ha^{-1}\,yr^{-1}$), the $C:N_{cr}$ in the microbial saturation model ranged narrowly from 25 to 29 across a range of clay concentrations (Fig. 4b). These results fall closely in line with traditional estimates of $C:N_{cr}$ that have been developed for relatively N rich residues (Sinsabaugh et al., 2013).

The addition of a microbial pool appears to be an important component of a C saturation model that allows it to accurately represent the short-term dynamics of N storage and turnover in microbial biomass. We were able to achieve this improvement while preserving estimates of C storage and at the cost of only one additional parameter to the model. This improvement results in a model structure that can be applied to a broader set of ecological processes including both C and N cycling at short and long time scales.

4.2 The influence of C saturation on N mineralization

The influence of C saturation on N mineralization dynamics depends on whether C saturation is modeled as a process regulating ε or k. In the single-pool and microbial saturation models, the C saturation ratio is used to regulate ε, coupling C saturation and N mineralization processes based on Eq. (1). In the abiotic saturation model, where the saturation ratio does not regulate ε but rather k, C saturation does not affect N mineralization dynamics. These differences in how the models simulate C saturation present contrasting hypotheses of how C saturation could affect N mineralization dynamics.

BGD
11, 9667–9695, 2014

If C saturation does indeed affect N mineralization, there may be important implications for ecosystem management. For example, increasing C inputs to an ecosystem to promote C sequestration in the soil would result in increased N mineralization and potentially increased N losses. Management practices that redistribute SOC concentrations in a soil profile and mix layers with higher saturation ratio (e.g. top layer in no-till systems) with layers of lower saturation, would result in altered N mineralization patterns from crop residues.

Despite these potential implications, few studies so far address the effects of C saturation on N mineralization dynamics. Castellano et al. (2012) presented a conceptual model linking C and N saturation theories which was supported by evidence that increasing levels of C saturation reduced the transfer of NH_4-N to mineral associated organic matter and increased potential net nitrification. Similarly, McLauchlan (2006) found that net N mineralization decreased as clay content increased in soils aggrading C following agricultural abandonment.

The findings of both of these studies are consistent with the behavior of the microbial saturation model where C saturation affects N mineralization dynamics, but not with the abiotic saturation model. Furthermore, behavior of the microbial saturation model is echoed by the non-saturation model RothC in the response of $C:N_{cr}$ across a clay gradient (Fig. 4b). Models that use f_{clay} to regulate ε directly introduce a similar dependency of N mineralization on soil texture as does the microbial saturation model. As discussed earlier, C saturation theory may be a more fundamental mechanism to explain the effects of soil texture on C and N cycling, and studies that demonstrated an influence of soil texture on N mineralization under a paradigm of non-saturation C models (Ladd et al., 1981; Van Veen et al., 1985; Schimel, 1986) may well be used to support the idea that C saturation affects N mineralization.

Although the currently limited data on the links between C saturation and N mineralization dynamics seem to support a coupling of these processes, it does not permit assessing with certainty the practical significance of such a relationship. For instance, at reasonable C input rates, the change in $C:N_{cr}$ due to the effects of a clay gradient

BGD
11, 9667–9695, 2014

on the C saturation ratio is rather minor in the microbial saturation model (e.g., 25 to 29 as in Fig. 4b). The effect of C saturation on $C:N_{cr}$ becomes much more pronounced as the saturation ratio increases above 0.5 (Fig. 4a). This level of saturation requires very high C inputs under the current parameterization of our model, but is easily achieved in the top layer of no-till soils or intact natural grasslands (Mazzilli et al., 2014). Clearly, it will require experimental work to assess whether these model predictions are attuned to observed patterns of N mineralization.

Given the limited but encouraging data supporting the conceptual and quantitative link between C saturation and N mineralization, we believe that further empirical research to test this link should be pursued. One new hypothesis generated by our work is that as C saturation ratio increases so does the $C:N_{cr}$ of decomposing plant residues. If this hypothesis is correct, further studies should evaluate its practical implications for managing C and N in natural and managed ecosystems. For example, are N mineralization dynamics altered by C saturation patterns in a soil profile such as those in no-till systems with stratified soil organic matter? We also suggest conducting additional studies to verify and improve our estimation of the maximum soil C storage capacity (C_x), as the quantitative relationship between C saturation and N mineralization is sensitive to this value and our current method of estimation is based on the results of only one study (Hassink and Whitmore, 1997).

5 Conclusions

We demonstrated that different C saturation model structures can produce similar predictions of C storage, but that predictions of N mineralization can diverge widely. Inclusion of a microbial pool in the C model led to reasonable predictions of N mineralization. We also demonstrated that the link between C saturation and N mineralization depends on whether C saturation is modeled as a process regulating transfer efficiencies or transfer rates among pools in the model. These findings lead to specific hypotheses about the relationship between C saturation and N mineralization that can be tested

BGD
11, 9667–9695, 2014

empirically, and offer a clear pathway to harmonize C saturation and N mineralization in biogeochemical models.

Appendix A:

Deriving the parameter k_s for the microbial saturation model that would force steady-state C_s levels to be equivalent to the single-pool saturation model required reformulating Eq. (4) to solve dC_s/dt with respect to C_r. This is achieved by solving steady-state Eq. (5) for $k_m C_m$ and substituting this for $k_m C_m$ in Eq. (4). The result is Eq. (A1):

$$dC_s/dt = \varepsilon^2 k_r C_r - (1 - \varepsilon^2) k_s C_s \quad \text{(A1)}$$

Equations (A1) and (3) can equated and the turnover rate for C_s in model B solved:

$$k_s = \frac{5.48 \times 10^{-5}}{(1 - \varepsilon^2)} \quad \text{(A2)}$$

To derive parameters for the abiotic saturation model that would force steady-state C_s levels to be equivalent to steady-state C_s levels in the single-pool saturation model we reformulated Eq. (6) to solve dC_s/dt with respect to C_r. This required rearrangements of Eqs. (7) and (8) along with several substitutions. First, steady-state Eq. (8) was solved for $k_m C_m$ and substituted into Eq. (7), which was then solved for C_{un}. The resulting equation for C_{un} was substituted into Eq. (6), yielding:

$$dC_s/dt = \varepsilon_r \varepsilon k_{un\text{-}s} k_r C_r - k_{un}(1 - \varepsilon_r \varepsilon) k_s C_s \quad \text{(A3)}$$

Equations (A3) and (3) can be equated and the decay rates $k_{un\text{-}s}$ and k_s solved:

$$k_{un\text{-}s} = \frac{\varepsilon_x (1 - C_s/C_x)}{\varepsilon \varepsilon_r} \quad \text{(A4)}$$

$$k_s = \frac{5.48 \times 10^{-5}}{k_{un}(1 - \varepsilon \varepsilon_r)} \quad \text{(A5)}$$

BGD
11, 9667–9695, 2014

References

Castellano, M., Kaye, J., Lin, H., and Schmidt, J.: Linking carbon saturation concepts to nitrogen saturation and retention, Ecosystems, 15, 175–187, 2012.

Hassink, J.: Preservation of plant residues in soils differing in unsaturated protective capacity, Soil Sci. Soc. Am. J., 60, 487–491, 1996.

Hassink, J. and Whitmore, A. P.: A model of the physical protection of organic matter in soils, Soil Sci. Soc. Am. J., 61, 131–139, 1997.

Hénin, S. and Dupuis, M.: Essai de bilan de la matière organique du sol, Ann. Agron., 15, 17–29, 1945.

Huggins, D. R., Clapp, C. E., Allmaras, R. R., Lamb, J. A., and Laysee, M. F.: Carbon dynamics in corn-soybean sequences as estimated from natural Carbon-13 abundance, Soil Sci. Soc. Am. J., 62, 195–203, 1998.

Jenkinson, D. S.: The turnover of organic-carbon and nitrogen in soil, Philos. T. R. Soc. B, 329, 361–368, 1990.

Kemanian, A. R. and Stöckle, C. O.: C-Farm: a simple model to evaluate the carbon balance of soil profiles, Eur. J. Agron., 32, 22–29, 2010.

Kemanian, A. R., Manoranjan, V. S., Huggins, D. R., and Stöckle, C. O.: Assessing the Usefulness of Simple Mathematical Models to Describe Soil Carbon Dynamics, 3rd USDA Symposium on Greenhouse Gases & Carbon Sequestration in Agriculture and Forestry, Baltimore, Maryland, 21–24 March 2005, 2005.

Kemanian, A. R., Julich, S., Manoranjan, V. S., and Arnold, J. R.: Integrating soil carbon cycling with that of nitrogen and phosphorus in the watershed model SWAT: theory and model testing, Ecol. Model., 222, 1913–1921, 2011.

Ladd, J. N., Oades, J. M., and Amato, M.: Microbial biomass formed from ^{14}C,^{15}N-labelled plant material decomposing in soils in the field, Soil Biol. Biochem., 13, 119–126, 1981.

Manzoni, S. and Porporato, A.: Soil carbon and nitrogen mineralization: theory and models across scales, Soil Biol. Biochem., 41, 1355–1379, 2009.

Manzoni, S., Jackson, R. B., Trofymow, J. A., and Porporato, A.: The global stoichiometry of litter nitrogen mineralization, Science, 321, 684–686, 2008.

Manzoni, S., Trofymow, J. A., Jackson, R. B., and Porporato, A.: Stoichiometric controls on carbon, nitrogen, and phosphorus dynamics in decomposing litter, Ecol. Monogr., 80, 89–106, 2010.

BGD
11, 9667–9695, 2014

Manzoni, S., Taylor, P., Richter, A., Porporato, A., and Ågren, G. I.: Environmental and stoichiometric controls on microbial carbon-use efficiency in soils, New Phytol., 196, 79–91, 2012.
Mazzilli, S., Kemanian, A., Ernst, O., Jackson, R., Piñeiro, G.: Priming of soil organic carbon decomposition induced by corn compared to soybean crops, Soil Biol. Biochem., 75, 273–281, 2014.
McLauchlan, K. K.: Effects of soil texture on soil carbon and nitrogen dynamics after cessation of agriculture, Geoderma, 136, 289–299, 2006.
Parton, W. J., Schimel, D. S., Cole, C. V., and Ojima, D. S.: Analysis of factors controlling soil organic matter levels in Great Plains grasslands, Soil Sci. Soc. Am. J., 51, 1173–1179, 1987.
Schimel, D. S.: Carbon and nitrogen turnover in adjacent grassland and cropland ecosystems, Biogeochemistry, 2, 345–357, 1986.
Sinsabaugh, R. L., Manzoni, S., Moorhead, D. L., and Richter, A.: Carbon use efficiency of microbial communities: stoichiometry, methodology and modelling, Ecol. Lett., 16, 930–939, 2013.
Sørensen, L. H.: The influence of clay on the rate of decay of amino acid metabolites synthesized in soils during decomposition of cellulose, Soil Biol. Biochem., 7, 171–177, 1975.
Sørensen, L. H.: Carbon–nitrogen relationships during the humification of cellulose in soils containing different amounts of clay, Soil Biol. Biochem., 13, 313–321, 1981.
Stewart, C. E., Paustian, K., Conant, R. T., Plante, A. F., and Six, J.: Soil carbon saturation: concept, evidence and evaluation, Biogeochemistry, 86, 19–31, 2007.
Van Veen, J. A., Ladd, J. N., and Amato, M.: Turnover of carbon and nitrogen through the microbial biomass in a sandy loam and a clay soil incubated with [^{14}C(U)] Glucose and [^{15}N] $(NH_4)_2SO_4$ under different moisture regimes, Soil Biol. Biochem., 17, 747–756, 1985.
Verberne, E. L. J., Hassink, J., Dewilligen, P., Groot, J. J. R., and Van Veen, J. A.: Modeling organic-matter dynamics in different soils, Neth. J. Agr. Sci., 38, 221–238, 1990.

BGD
11, 9667–9695, 2014

Table 1. The parameter values used in each model.

Parameter	Units	Single-pool Saturation	Microbial Saturation	Abiotic Saturation	RothC
C_x [a]	g C kg^{-1} soil	$21.1 + 37.5 f_{clay}$	$21.1 + 37.5 f_{clay}$	$21.1 + 37.5 f_{clay}$	
ε_x	g C g^{-1} C	0.18	0.18	0.18	
ε	g C g^{-1} C	$\varepsilon_x(1 - C_s/C_x)$	$\sqrt{\varepsilon_x(1 - C_s/C_x)}$	0.25	$\frac{1}{4.09+2.67e^{-7.86 f_{clay}}}$
ε_r	g C g^{-1} C			0.75	
k_r	d^{-1}	0.0165	0.0165	0.0165	
k_{dpm}	d^{-1}				0.0274
k_{rpm}	d^{-1}				8.2×10^{-4}
k_s	d^{-1}	5.48×10^{-5}	$\frac{5.48\times10^{-5}}{(1-\varepsilon^2)}$	$\frac{5.48\times10^{-5}}{k_{un}(1-\varepsilon\varepsilon_r)}$	5.48×10^{-5}
k_m	d^{-1}		1.81×10^{-3}	1.81×10^{-3}	1.81×10^{-3}
$k_{un\text{-}s}$	d^{-1}			$\frac{\varepsilon_x(1-C_s/C_x)}{\varepsilon\varepsilon_r}$	
k_{un}	d^{-1}			0.01	

[a] C_x as calculated by Hassink and Whitmore (1997). For use in the modeling exercises, we converted C_x to units of Mg C ha^{-1} by assuming a soil bulk density of 1.3 Mg m^{-3} and a soil depth of 0.3 m.
[b] f_{clay} is the clay concentration (g clay g^{-1} soil).

BGD
11, 9667–9695, 2014

Table 2. Differential equations for carbon pools in each model.

Single-pool saturation model	
$dC_s/dt = \varepsilon k_r C_r - k_s C_s$	(3)
Microbial saturation model	
$dC_s/dt = \varepsilon k_m C_m - k_s C_s$	(4)
$dC_m/dt = \varepsilon k_r C_r + \varepsilon k_s C_s - k_m C_m$	(5)
Abiotic saturation model	
$dC_s/dt = k_{un\text{-}s} C_{un} - k_s C_s$	(6)
$dC_{un}/dt = \varepsilon_r k_m C_m + k_s C_s - k_{un} C_{un} - k_{un\text{-}s} C_{un}$	(7)
$dC_m/dt = \varepsilon k_r C_r + \varepsilon k_{un} C_{un} - k_m C_m$	(8)
RothC	
$dC_s/dt = 0.54\varepsilon(k_{dpm} C_{dpm} + k_{rpm} C_{rpm} + k_m C_m + k_s C_s) - k_s C_s$	(9)
$dC_m/dt = 0.46\varepsilon(k_{dpm} C_{dpm} + k_{rpm} C_{rpm} + k_m C_m + k_s C_s) - k_m C_m$	(10)

BGD
11, 9667–9695, 2014

Table 3. Analytical solutions to the steady-state level of the SOC pools in each model. Input rates C_r, C_{rpm}, and C_{dpm} and turnover rates k_s, k_m, and k_{un} should be expressed in the same time units.

All saturation models

$$C_s = \frac{\varepsilon_x C_r}{k_s^* + \varepsilon_x C_r / C_x} \quad (12)$$

Microbial saturation model

$$C_m = \frac{\sqrt{\varepsilon_x (1 - C_s/C_x)} C_r}{k_m (1 - \varepsilon_x (1 - C_s/C_x))} \quad (13)$$

Abiotic saturation model

$$C_m = \frac{\varepsilon C_r}{k_m (1 - \varepsilon \varepsilon_r)} \quad (14)$$

$$C_{un} = \frac{\varepsilon \varepsilon_r C_r}{k_{un} (1 - \varepsilon \varepsilon_r)} \quad (15)$$

RothC

$$C_s = \frac{0.54 \varepsilon (C_{dpm} + C_{rpm})}{k_s (1 - \varepsilon)} \quad (16)$$

$$C_m = \frac{0.46 \varepsilon (C_{dpm} + C_{rpm})}{k_m (1 - \varepsilon)} \quad (17)$$

* The k_s parameter value from the single-pool saturation model.

BGD
11, 9667–9695, 2014

Table 4. The analytical solution to $C:N_{cr}$ in each model.

Single-pool saturation	
$C:N_{cr} = \frac{C:N_s}{\varepsilon_x(1-C_s/C_x)}$	(18)
Microbial saturation	
$C:N_{cr} = \frac{C:N_m}{\sqrt{\varepsilon_x(1-C_s/C_x)}}$	(19)
Abiotic saturation	
$C:N_{cr} = \frac{C:N_m}{0.25}$	(20)
RothC	
$C:N_{cr} = C:N_m(4.0 + 2.67e^{-7.86f_{clay}})$	(21)

BGD
11, 9667–9695, 2014

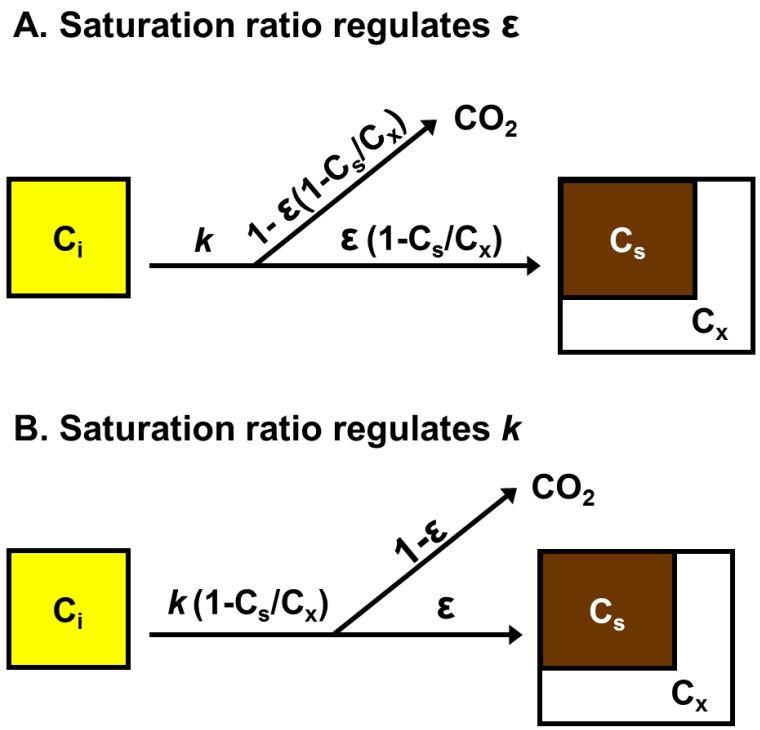

Figure 1. Conceptual models illustrating two different methods of implementing C saturation dynamics. In both models, the C saturation ratio of the saturating pool is defined by the ratio of the current pool size (C_s) to a theoretical maximum pool size (C_x), or C_s/C_x. In model A, the C saturation ratio regulates the C transfer efficiency (ε) between the donor pool (C_i) and C_s. As the C saturation ratio increases, less of the C decomposed from C_i is transferred to C_s and more is respired as CO_2. In model B, the C saturation ratio regulates the decomposition rate (k) of C_i, such that the rate decreases as the C saturation ratio increases. The C transfer efficiency is not affected by the C saturation ratio in model B.

BGD
11, 9667–9695, 2014

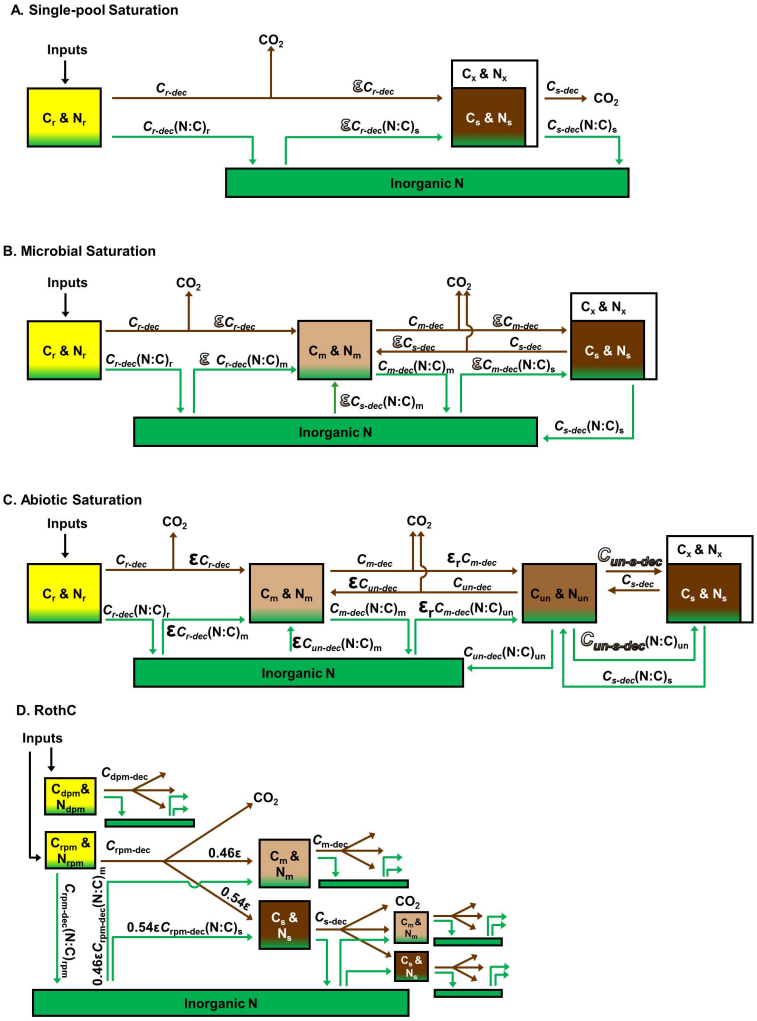

BGD
11, 9667–9695, 2014

Implications of C saturation model structure for N mineralization dynamics

C. M. White et al.

Figure 2. Diagrams of the pools and fluxes in the four models used in this study. Carbon and N pools are indicated together in boxes. Carbon fluxes are indicated by brown arrows and N fluxes by green arrows. Pools are abbreviated as follows: C_r, C_{dpm}, C_{rpm} and N_r, N_{dpm}, N_{rpm} are plant residues; C_m and N_m are microbial biomass; C_{un} and N_{un} are un-protected soil organic matter; C_s and N_s are protected or stabilized soil organic matter; C_x and N_x are the maximum or saturating capacity for C and N storage. The inorganic N pool is represented by a green box. Carbon decomposition from each pool and the pool stoichiometry are represented by the symbols $C_{j\text{-dec}}$ and $(N:C)_j$, respectively, where j specifies the pool. Pools decompose with first order kinetics based on rates listed in Table 1. The symbol ε is the C transfer efficiency to the receiving pool, the value of which is specified by Table 1 for each model. Symbols illustrated with a brown gradient fill pattern are regulated by the C saturation ratio (C_s/C_x).

BGD
11, 9667–9695, 2014

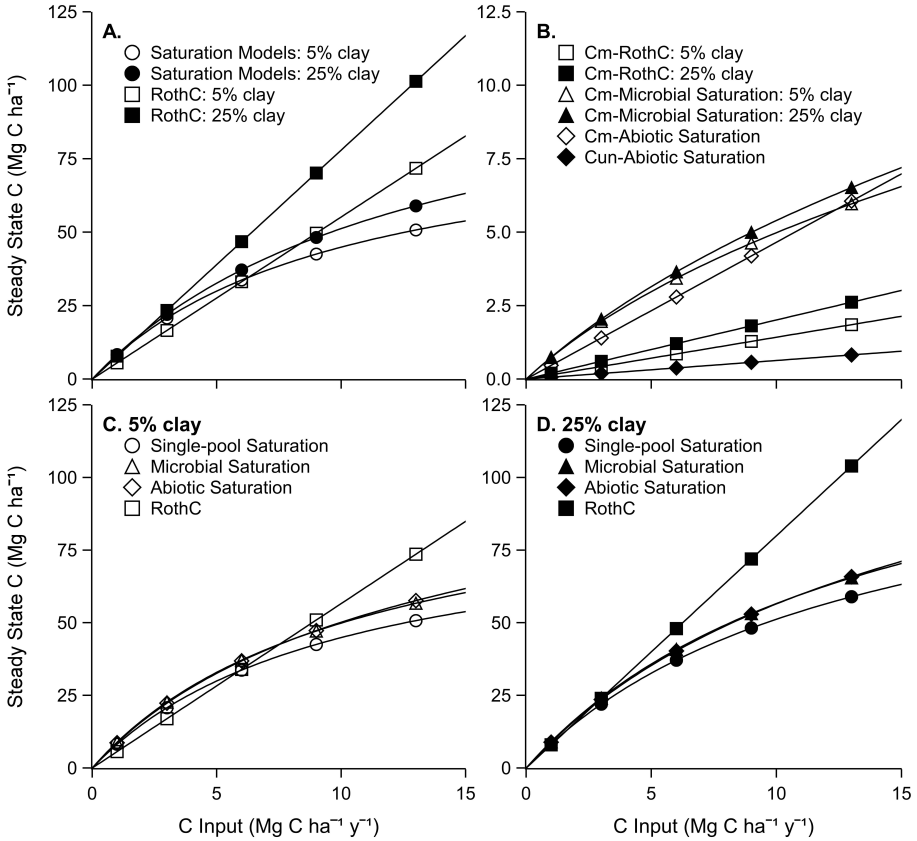

Figure 3. The relationship between C input level and the steady-state C level of various pools in each model for soils with contrasting clay concentration. **(A)** The C_s pool of each model in soils with 5 % and 25 % clay concentration. **(B)** Other C pools in each model in soils with 5 % and 25 % clay concentration (note: the pools in the abiotic saturation model are not sensitive to clay concentration). **(C, D)** The total SOC pool size in soils with 5 % clay **(C)** and 25 % clay **(D)**.

BGD
11, 9667–9695, 2014

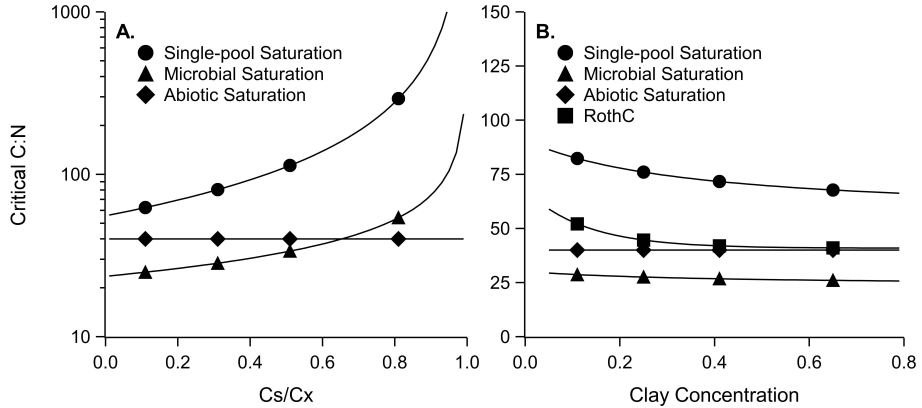

Figure 4. $C:N_{cr}$ as a function of carbon saturation ratio **(A)** and clay concentration **(B)**. In **(B)**, the pool size for C_s was maintained constant at 32 Mg C ha^{-1}, thus the clay gradient creates a C saturation gradient. For reference, a pool size of 32 Mg C ha^{-1} would result from an annual C input level of $\sim$ 5 Mg C ha^{-1} yr^{-1}.

BGD
11, 9667–9695, 2014

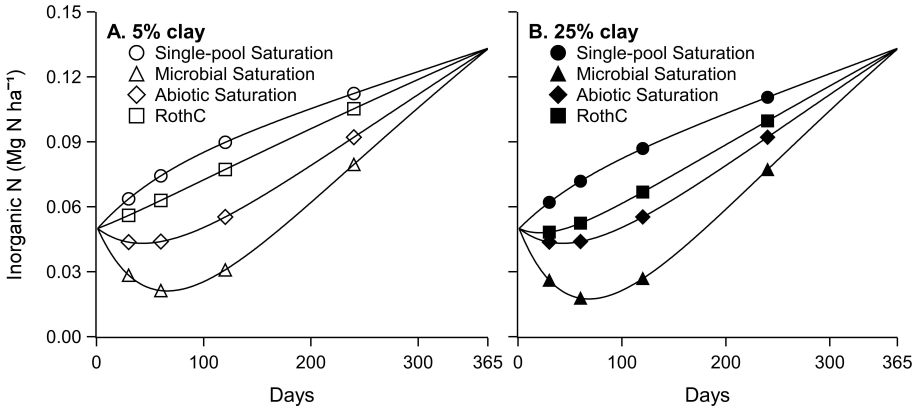

Figure 5. The inorganic N pool during decomposition of a 5 Mg C ha^{-1} residue addition with a C : N of 60 in a soil with 5 % clay concentration **(A)** and 25 % clay concentration **(B)**. Soil C pool sizes for each model structure were initialized to the steady state levels that would occur from annual residue additions of 5 Mg C ha^{-1}. Residue and soil C pools decomposed at the optimum rates listed in Table 1.

BGD
11, 9667–9695, 2014